The EMBO Journal Vol. 21 No. 7 pp. 1535–1544, 2002

Lack of collagen XVIII/endostatin results in eye abnormalities

Naomi Fukai, Lauri Eklund[1], Alexander G.Marneros, Suk Paul Oh[2], Douglas R.Keene[3], Lawrence Tamarkin[4], Merja Niemelä[1], Mika Ilves[5], En Li[6], Taina Pihlajaniemi[1] and Bjorn R.Olsen[7]

Department of Cell Biology, Harvard Medical School, Boston, MA 02115, USA, [1]Collagen Research Unit, Biocenter and Department of Medical Biochemistry, University of Oulu, Oulu, FIN-90014, Finland, [2]Department of Physiology, University of Florida, Gainesville, FL 32610, [3]Portland Imaging Center, Shriners Hospitals for Children, Portland, OR 97201, [4]CytImmune Sciences, Inc., College Park, MD 20740, [5]Biocenter and Department of Physiology, University of Oulu, FIN-90014, Finland and [6]Cardiovascular Research Division of Massachusetts General Hospital, Boston, MA 02114, USA

[7]Corresponding author
e-mail: bjorn_olsen@hms.harvard.edu

N.Fukai, L.Eklund and A.G.Marneros contributed equally to this work

Mice lacking collagen XVIII and its proteolytically derived product endostatin show delayed regression of blood vessels in the vitreous along the surface of the retina after birth and lack of or abnormal outgrowth of retinal vessels. This suggests that collagen XVIII/endostatin is critical for normal blood vessel formation in the eye. All basement membranes in wild-type eyes, except Descemet's membrane, showed immunogold labeling with antibodies against collagen XVIII. Labeling at sites where collagen fibrils in the vitreous are connected with the inner limiting membrane and separation of the vitreal matrix from the inner limiting membrane in mutant mice indicate that collagen XVIII is important for anchoring vitreal collagen fibrils to the inner limiting membrane. The findings provide an explanation for high myopia, vitreoretinal degeneration and retinal detachment seen in patients with Knobloch syndrome caused by loss-of-function mutations in collagen XVIII.

Keywords: collagen XVIII/endostatin/eye abnormalities/immunogold labeling/knockout mice

Introduction

Collagen XVIII, expressed as three variants with differences in their N-terminal regions but sharing multiple triple-helical domains separated by non-triple-helical regions, is a proteoglycan located in basement membranes of epithelia and vascular endothelium (Oh *et al*., 1994; Rehn and Pihlajaniemi, 1994; Muragaki *et al*., 1995; Halfter *et al*., 1998; Saarela *et al*., 1998). Part of the C-terminal non-triple-helical (NC1) domain of collagen XVIII, common to all variants, represents the anti-angiogenic fragment named endostatin (O'Reilly *et al*., 1997). Endostatin is separated from an upstream trimerization region by a protease-sensitive hinge (Sasaki *et al*., 1998). Cleavage within the hinge results in release of endostatin and endostatin-like fragments that can be detected in blood plasma and tissue extracts (Sasaki *et al*., 1998). Cathepsin L and matrix metalloproteases (MMPs) can cleave within the hinge (Felbor *et al*., 2000); other enzymes may also play a role in the generation of endostatins during physiological or pathological processing of collagen XVIII (Wen *et al*., 1999; Ferreras *et al*., 2000).

It has been proposed that collagen XVIII/endostatin may function to act as a local basement membrane-associated regulator of angiogenesis during processes that result in release of cathepsins and metalloproteinases (Felbor *et al*., 2000). It is also likely that the triple-helical, heparan sulfate-containing portion of collagen XVIII plays a role in the assembly, maintenance, structural integrity or cellular binding properties of basement membranes. In fact, the discovery that Knobloch syndrome, in a Brazilian pedigree, is caused by a splice site mutation affecting the short form of collagen XVIII (Sertié *et al*., 2000) supports a structural function for collagen XVIII. In Knobloch syndrome, affected individuals develop high myopia, vitreoretinal degeneration with retinal detachment, macular abnormalities and a localized defect in the occipital region of the skull described (somewhat inappropriately) as occipital encephalocele. Apart from the macular abnormalities and encephalocele, these are features that are also seen in Stickler-like syndromes as a result of mutations in *COL2A1* or *COL11A1* genes (Mundlos and Olsen, 1997; Annunen *et al*., 1999). Since collagen XVIII is expressed in the developing and postnatal eye (Sasaki *et al*., 1998; Halfter *et al*., 2000), along with collagens II and XI, it is possible that this non-fibrillar collagen is part of a tissue scaffold that is essential for maintaining a normal vitreous structure and functional retina.

The phenotypic consequences of a complete lack of collagen XVIII support this possibility. In mice with *Col18a1* null alleles, ocular abnormalities include a delay in normal postnatal regression of hyaloid vessels along the inner limiting membrane of the retina [vasa hyaloidea propria (VHP)] and abnormal outgrowth of the retinal vasculature. Lack of collagen XVIII/endostatin also causes alterations along the inner limiting membrane at the vitreous/retina interphase. The results are consistent with the hypothesis that collagen XVIII/endostatin is critical for the function of basement membranes in specific anatomical locations, and we suggest that the alterations provide an explanation for the ocular abnormalities of patients with Knobloch syndrome.

Results

No expression of collagen XVIII/endostatin and no gross abnormalities in mice with targeted Col18a1 alleles

DNA for the targeting vector was from a genomic fragment containing exons 17–38 of *Col18a1* (Figure 1A). A *Sal*I site within exon 30 was used to insert a *neo*^{R} cassette to generate a replacement vector (Figure 1B). In this position, the *neo*^{R} cassette would interrupt all variant forms of collagen XVIII. Homologous recombination was confirmed by Southern blots using an *Eco*RI–*Kpn*I fragment as probe (data not shown) and by PCR (Figure 1C). PCR was used for subsequent genotyping since PCR results were in complete agreement with Southern analyses.

Northern blots of RNAs from embryonic and adult tissues of homozygous mutants failed to reveal detectable levels of α1(XVIII) mRNA. In contrast, RNAs from wild-type embryos and adult livers showed high levels of α1(XVIII) expression, and RNAs from heterozygous embryos showed about half the levels of wild-type mice (Figure 1D). Determination of circulating levels of collagen XVIII-derived fragments in plasma of wild-type, heterozygous and homozygous animals showed no detectable endostatin or endostatin-like fragments in homozygous null mice. Heterozygotes had levels that were 50% of those of wild-type animals (23.4 ± 2.7 versus 44.9 ± 7.5 ng/ml). Northern blots with a probe covering exons 4–7 from the 5′ region of *Col18a1* and immunohistochemistry of homozygous null tissues with an antibody against the NC11(XVIII) domain (see below) were completely negative, proving that shorter transcripts representing the 5′ region of *Col18a1* and their protein products are not expressed in null animals.

No gross abnormalities were detected by inspection of mutant embryos or adult animals. Mating of homozygotes indicated no reduction in reproductive capacity, and 43 consecutive matings between heterozygotes gave the expected ratios of offspring, namely 89 wild type, 174 heterozygotes and 92 homozygotes. Light microscopy revealed no abnormalities in the mutant mice. We paid particular attention to the vascularity of tissues and the structure of basement membrane-containing regions of

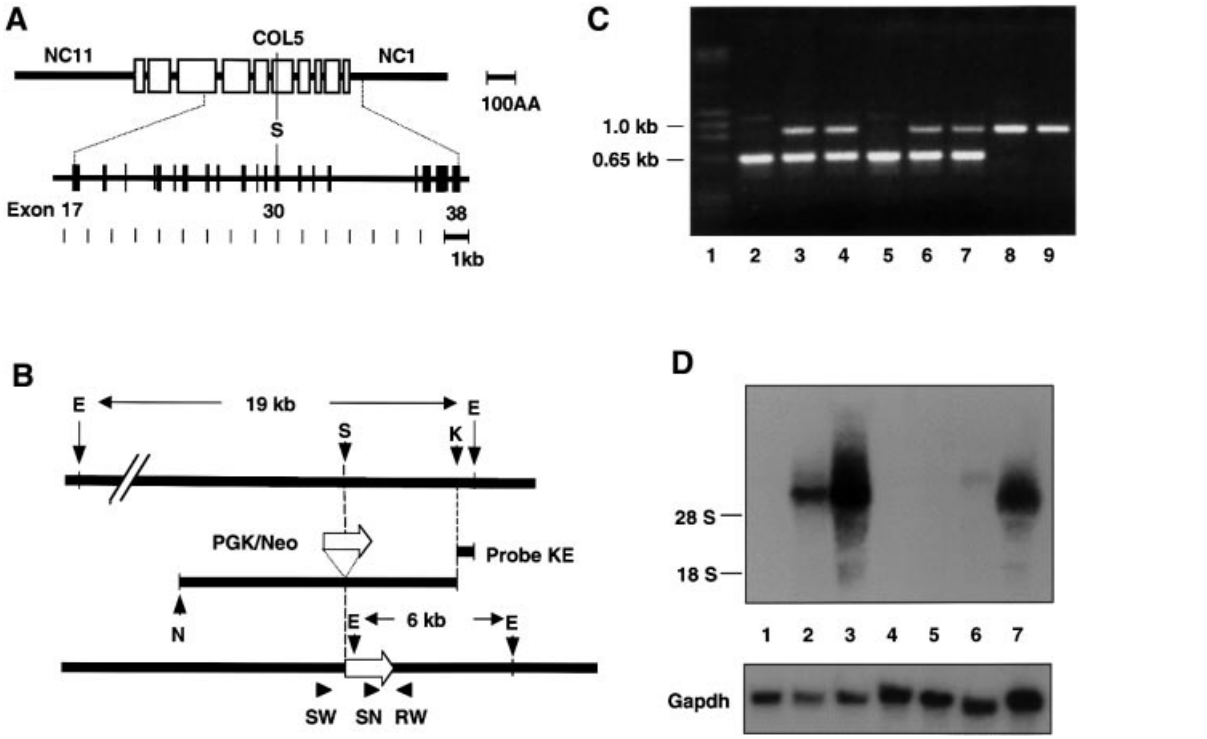

Fig. 1. (**A**) Diagram showing domain structure of α1(XVIII) collagen (top) and exon structure of central portion of *Col18a1* gene (bottom). Size markers [in 100 amino acid (AA) and 1 kb units] are shown at right. Triple-helical domains are indicated by open boxes, and non-triple helical protein domains by a heavy line. Non-triple helical domains at carboxyl and amino ends are labeled NC1 and NC11, respectively. Exons are represented by vertical bars and introns by a line. A unique *Sal*I site (S), in exon 30, corresponds to site within COL5 domain, used for insertion of *neo*^{R} cassette in targeting construct. (**B**) Diagram showing targeting construct (middle) and its relationship to wild-type gene (top) and targeted gene following homologous recombination (bottom). Open arrow indicates the direction of transcription of *PKG/Neo* gene. Probe KE was used for screening ES cell clones. Southern blotting with this probe detects a 19 kb *Eco*RI fragment in wild-type DNA and a 6 kb *Eco*RI fragment in targeted DNA. Primers (SW, SN and RW) and their directions (arrowheads) used for PCR-based genotyping are shown at the bottom. E, *Eco*RI; S, *Sal*I; K, *Kpn*I; N, *Not*I. (**C**) Gel electrophoresis of PCR products with mouse tail DNA and primer pairs SW/RW and SN/RW. Lane 1, size markers; lanes 2 and 5, DNA from homozygous *Col18a1* null mice; lanes 3, 4, 6 and 7, DNA from heterozygous mice; lanes 8 and 9, DNA from wild-type mice. Sizes of PCR products indicated on the left. (**D**) Northern blot probed for *Col18a1* with RNA from wild-type, heterozygous and homozygous mutant mice. The probe was from 3′ untranslated and endostatin region of mRNA. Lanes 1, 4, 5 and 6, RNA from homozygous *Col18a1* null mice; lane 2, RNA from heterozygous *Col18a1*$^{+/-}$ mouse; lanes 3 and 7, RNA from wild-type mice. In lanes 1–4 RNA from adult liver; in lane 5 from adult lung; in lane 6 from adult kidney; in lane 7 from embryonic day 17.5 whole embryos. Results of reprobing the blot for *Gapdh* are shown at the bottom. Positions of 18S and 28S RNAs are indicated on the left.

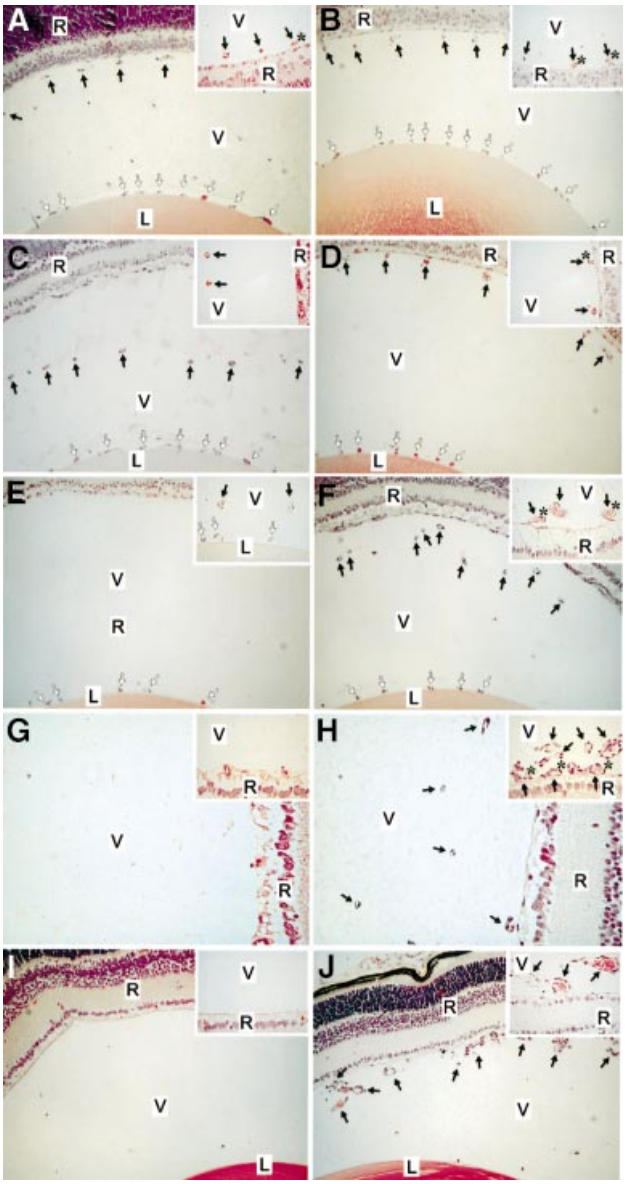

Fig. 2. Delayed regression of hyaloid capillaries in *Col18a1*$^{-/-}$ mice compared with age-matched wild-type mice at postnatal days 0.5 (A, B), 4 (C, D), 8 (E, F), 16 (G, H) and 24 (I, J). Abbreviations: L, lens; V, vitreous; R, retina. Symbols: black arrows, hyaloid capillaries; white arrows, TVL; asterisk, contact between hyaloid capillary and retina. Original magnifications: (A–F), (I) and (J), ×40; (G) and (H), ×80; all insets, ×160. Horizontal sections through eye of wild-type (**A**) and *Col18a1*$^{-/-}$ mouse (**B**) at postnatal day 0.5 showing transverse sections of hyaloid capillaries at internal surface of retina and vessel branches attached to lens capsule (TVL). Insets: few vessels attached to surface of retina in wild-type mice, but were seen more frequently in *Col18a1*$^{-/-}$ mice. Hyaloid capillaries are clearly dissociated from retinal surface and start to show signs of regression in wild-type mice at day 4 (**C**). Hyaloid capillaries still near retina in *Col18a1*$^{-/-}$ mice (**D**) or in contact with it [(D), inset]. Hyaloid capillaries have disappeared from vitreous (**E**) or some rudiments can be seen in the vicinity of the lens [(E), inset] in wild-type eyes at postnatal day 8. In age-matched *Col18a1*$^{-/-}$ mice, hyaloid capillaries are found within vitreous (**F**), near or attached to retina [(F), inset]. In some *Col18a1*$^{-/-}$ capillaries the diameter is increased and numerous erythrocytes [(F), inset] are seen. Hyaloid capillaries were completely removed from vitreous in wild-type mice at day 16 (**G**). In *Col18a1*$^{-/-}$ mice, hyaloid vessels still present in vitreous (**H**). Some persistent vessels are still connected to retina [(H), inset]. No hyaloid capillaries were found in 24-day-old wild-type mice (**I**). Most sections from *Col18a1*$^{-/-}$ eyes are comparable to wild-type samples; however, some sections show numerous persistent and enlarged vessels in vitreous (**J**).

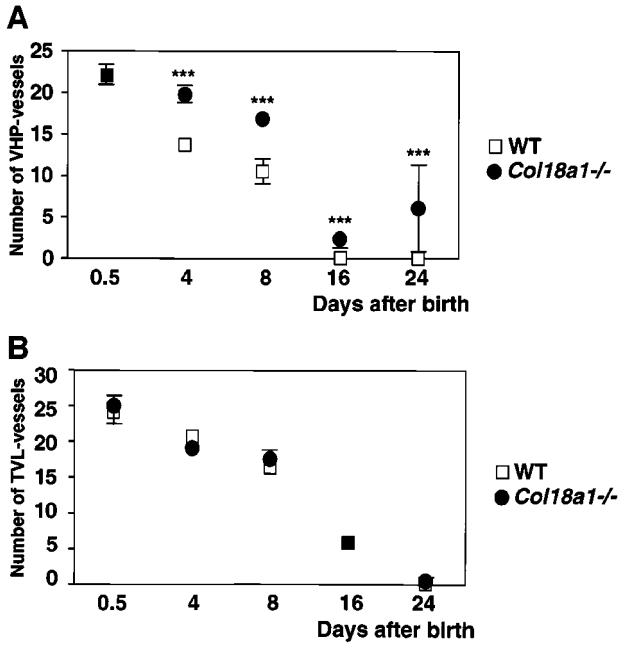

Fig. 3. The number of hyaloid vessel profiles in vitreous (**A**) and TVL (**B**) at different days in sections from wild-type (open squares, WT) and homozygous *Col18a1*$^{-/-}$ null (filled circles) mice. At each time point means of data from eight wild-type and nine *Col18a1*$^{-/-}$ mice are shown. Standard errors of the mean are indicated by vertical bars; significant differences between wild-type and knockout values are indicated by triple asterisks.

various organs, but no morphological differences between wild-type and mutant mice were detected in organs such as heart, lungs, liver and kidney (not shown). Careful examination of the eye, however, showed differences between homozygous and wild-type/heterozygous animals in the regression of hyaloid vessels (VHP) after birth and in the postnatal outgrowth of retinal vessels.

Delayed regression of hyaloid vessels in collagen XVIII null mice

The vessels around the lens capsule [tunica vasculosa lentis (TVL)] and the VHP in the vitreous along the inner limiting membrane of the retina were examined in homozygous mutant mice and wild-type controls at postnatal days 0.5, 4, 8, 16 and 24. As shown in Figure 2, hyaloid vessels were clearly dissociated from the retinal surface and started to show signs of regression in wild-type mice at day 4 (Figure 2C); about half were left at day 8 (Figure 2E), and they were practically gone by postnatal day 16 (Figure 2G). No VHP capillaries were seen in the vitreous at day 24 in wild-type mice (Figure 2I). In contrast, the VHP in *Col18a1*$^{-/-}$ animals were still present near the retina at days 4 and 8, and persisted even at day 16 (Figure 2D, F and H). At day 24, most sections of homozygous mutants showed no VHP, but some sections still showed numerous and enlarged vessels in the vitreous (Figure 2J).

This delay in regression of the VHP in *Col18a1*$^{-/-}$ mice was evident from counting profiles of the hyaloid vasculature in sections from wild-type and mutant mice (Figure 3A). At postnatal day 0.5, there was no difference in the number of profiles between the two types of mice, but at all subsequent days examined, *Col18a1*$^{-/-}$ mice had

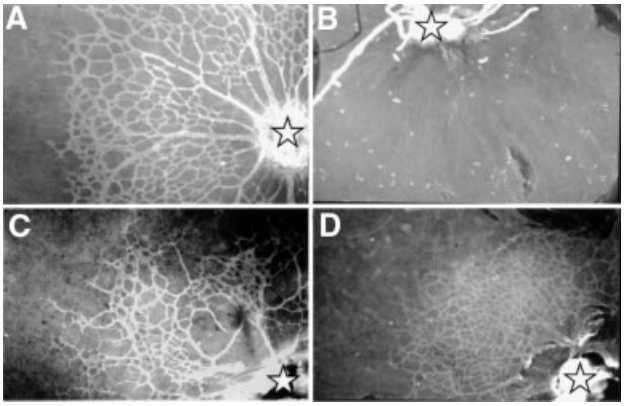

Fig. 4. Blood vessels in retinas of 4-day-old mice. Whole-mount immunofluorescence with antibodies against collagen IV in wild-type (**A**) and *Col18a1*$^{-/-}$ (B–D) mice, showing irregular development of blood vessels from optic nerve head (asterisks). In some *Col18a1*$^{-/-}$ samples there are no developing vessels (**B**), in some cases irregular growth of retinal capillaries (**C**), and in some, samples denser growth of capillaries (**D**) when compared with wild-type samples (A). Original magnification ×120.

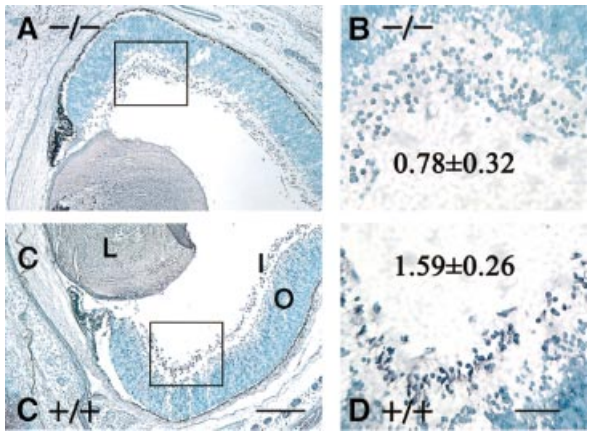

Fig. 5. Expression of VEGF by *in situ* hybridization in retinal neuroglia of collagen XVIII null [–/– (**A** and **B**)] and wild-type [+/+ (**C** and **D**)] eyes. Rectangular areas in (A) and (C) are shown at a higher magnification in (B) and (D). Relative levels of VEGF (±SD, $n = 4$) by quantitative PCR shown in (B) and (D). C, cornea; L, lens; I, inner cell layer; O, outer cell layer. Scale bars: (B), 200 μm; (D), 50 μm.

significantly more profiles in the vitreous than wild-type mice. In contrast to the differences seen between mutant and wild-type animals in the regression of the VHP, no differences were observed in the regression of vessels in the TVL (Figure 3B). Also, no differences were observed in the number and appearance of macrophages (hyalocytes) in the vitreous of mutant and wild-type animals.

Delayed and abnormal outgrowth of retinal vessels in collagen XVIII null mice

Examination of retinal vessels by immunofluorescent staining of whole mounts with collagen IV antibodies showed poor or irregular growth of capillaries in the retina of *Col18a1*$^{-/-}$ mice. In comparing 18 wild-type eyes with 55 *Col18a1*$^{-/-}$ eyes (Figure 4), 43.6% of the *Col18a1*$^{-/-}$ eyes did not show any or only very few short vessels in the retina (Figure 4B); 40% of *Col18a1*$^{-/-}$ eyes showed some, but fewer, vessels than wild-type eyes (Figure 4C); in 16.4%, the vessel outgrowth was comparable to that of wild-type eyes. Among the 40% with some, but fewer, vessels than wild-type eyes, focal areas of unusually dense capillary growth were seen in about half the samples (Figure 4D).

Reduced expression of VEGF in retinas of collagen XVIII null mice

The postnatal vascularization of the rodent retina is driven by hypoxia-induced vascular endothelial growth factor (VEGF) expression in neuroglial cells, and altering this expression causes abnormalities in vascular outgrowth (Alon *et al*., 1995; Stone *et al*., 1995; Benjamin *et al*., 1998; Yancopoulos *et al*., 2000). We therefore asked whether the abnormality in vessel outgrowth in collagen XVIII null eyes was associated with lack of VEGF up-regulation in neuroglial cells as a result of the persistence of VHP along the retinal surface. As shown in Figure 5, VEGF expression was less intense in neuroglial cells of *Col18a1*$^{-/-}$ than of wild-type eyes, as shown by *in situ* hybridization, and quantitative PCR demonstrated that

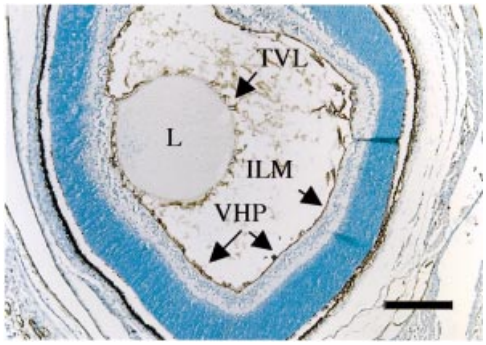

Fig. 6. Staining of wild-type mouse eye at postnatal day 1 with anti-collagen XVIII antibodies. Positive staining of basement membranes in TVL, around lens (L) and in VHP along inner limiting membrane (ILM). Scale bar, 200 μm.

the level of *VEGF* transcripts was ~50% lower in retinas of 4-day-old mutant than of wild-type mice (Figure 5).

Expression of collagen XVIII in the developing and postnatal eye

During the embryonic period, staining was seen in the basement membrane on the outside of the retina and of the inner limiting membrane with antibodies against the NC11(XVIII) domain. Staining was also seen of the basement membranes of VHP, of vessels in the TVL and of the lens capsule (Figure 6). In adult wild-type mice, immunofluorescence with antibodies against NC11(XVIII) showed reactivity in the iris basement membranes, lens capsule, inner limiting membrane and Bruch's membrane (Figure 7), but there was no staining of Descemet's membrane (not shown). The fact that there was no staining of any structure in eyes from homozygous *Col18a1*$^{-/-}$ mice demonstrated that the antibody is specific for collagen XVIII. Strong staining of the lens capsule, vessels in the TVL and the hyaloid capillaries was seen with antibodies against collagen IV, both in wild-type eyes and in eyes from homozygous collagen XVIII null mice at late embryonic stages (not shown).

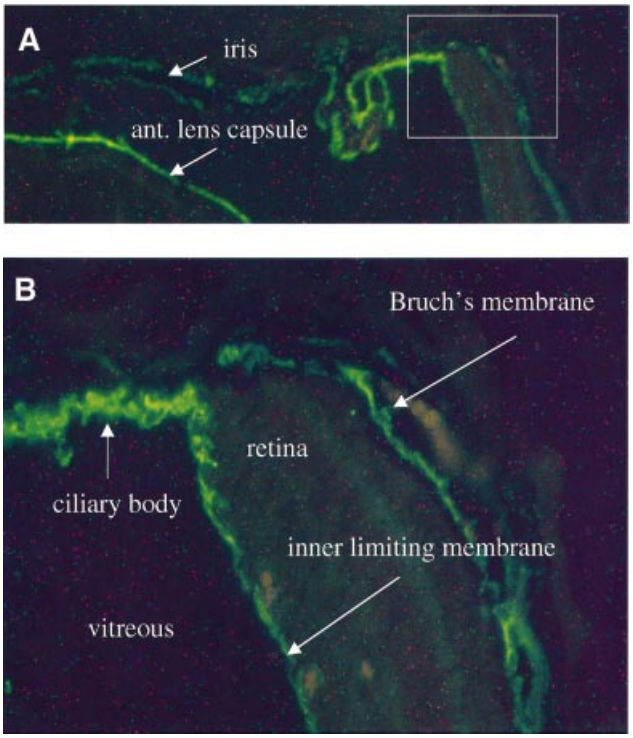

Fig. 7. Immunofluorescence staining of anterior portion of adult wild-type mouse eye with anti-collagen XVIII antibodies. Basement membranes of iris and anterior lens capsule are indicated in (**A**). Rectangular area in (A), shown at a higher magnification in (**B**), shows staining of basement membrane of ciliary body, inner limiting membrane and Bruch's membrane. Original magnification: (A), ×100; (B), ×400.

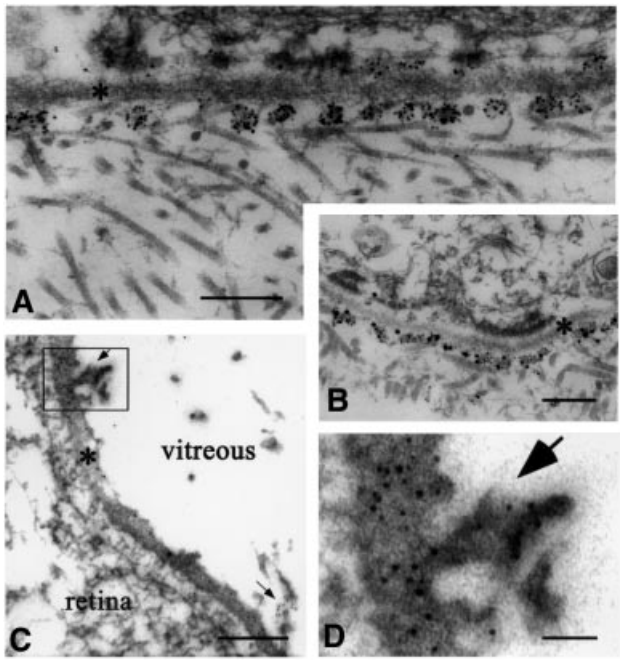

Fig. 8. Labeling of ocular and epidermal basement membranes of wild-type mice with gold-labeled anti-collagen XVIII antibodies. (**A**) Clusters of gold particles on matrix side (with collagen fibrils) along lamina densa (asterisk) of Bowman's membrane (scale bar 200 nm). Occasional clusters also on epithelial side. (**B**) Labeling of lamina densa (asterisk) along epidermal basement membrane (scale bar 400 nm); occasional larger particles, which are products of post-labeling enhancement, are visible. (**C**) Labeling of lamina densa (asterisk) of inner limiting membrane (scale bar 200 nm). Arrows indicate clusters of gold particles at sites where vitreal collagen fibrils approach inner limiting membrane. These particles are clearly evident in (**D**) (scale bar 50 nm), which shows the rectangular area in (C) at a higher magnification.

Ultrastructural location of collagen XVIII/ endostatin in ocular basement membranes

The presence of collagen XVIII in the basement membranes of the eye was confirmed by electron microscopy with gold-labeled antibodies against NC11(XVIII). Labeling was associated with Bowman's membrane of the cornea (Figure 8A), the inner limiting membrane (Figure 8C) and Bruch's membrane (Figure 9). In Bowman's membrane (Figure 8A), gold particles were distributed in clusters on the matrix side of the lamina densa, similar to what was found for epidermal basement membranes (Figure 8B). A similar clustering was seen in the iris (not shown) and along capillary basement membranes in Bruch's membrane (Figure 9A). In Bowman's membrane, the epidermal basement membrane and the capillary basement membrane, the clusters of labeled NC11(XVIII) domains appeared to be co-localized with fibrillar structures in the adjacent matrix, suggesting a role for collagen XVIII as a component of an anchoring complex between the fibrillar matrix and basement membranes. Along the inner limiting membrane, the gold particles were localized within the lamina densa and were clearly restricted to regions where vitreous fibrils are in close proximity to the membrane (Figure 8C and D). The difference in the localization of gold particles in the inner limiting membrane and epidermal/vascular basement membranes suggests a difference in the precise relationship of collagen XVIII to other components in the two types of basement membrane, but the co-localization with collagen fibrils supports the possibility of an anchoring function in both cases.

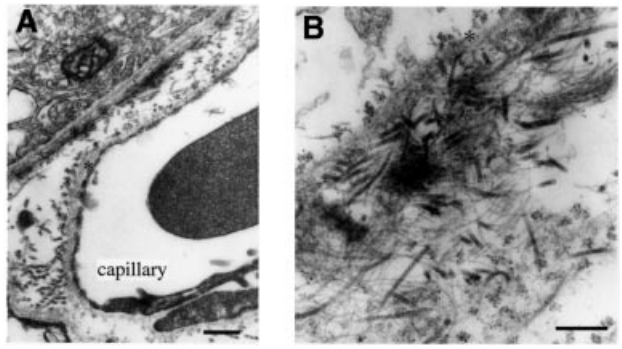

Fig. 9. Immunolabeling of Bruch's membrane with gold-labeled antibodies against collagen XVIII. (**A**) Low magnification overview (scale bar 400 nm) shows pigment epithelium in upper left-hand corner, capillary of choriocapillaris at lower right, and clusters of gold particles along lamina densa (asterisks) of epithelial and endothelial basement membranes; label is also seen associated with collagen fibrils in the space between the two basement membranes. (**B**) Tangential section through Bruch's membrane shown at a higher magnification (scale bar 250 nm). Clusters of gold particles seen on each side of lamina densa (asterisk) of pigment epithelial cells in upper left-hand corner. At the lower right, clusters of particles seen associated with collagen fibrils. Microfibrils and associated electron-dense material (probably elastin) in central area show little or no labeling.

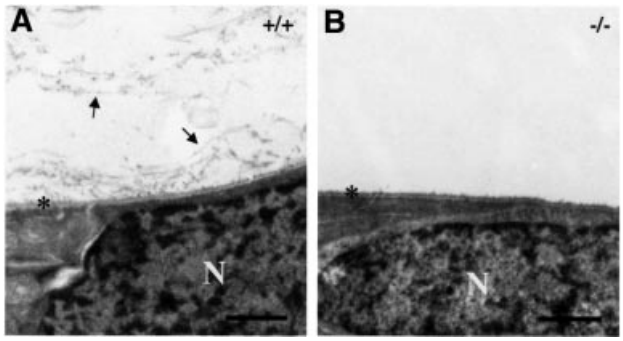

Fig. 10. Ultrastructure of retinal surface and adjacent vitreous in adult wild-type [+/+, (**A**)] and collagen XVIII null [–/–, (**B**)] mice. Lamina densa of inner limiting membrane is indicated by asterisks. Arrows, vitreal collagen fibrils in wild-type eye; N, nuclei of retinal cells. Scale bar, 1000 nm.

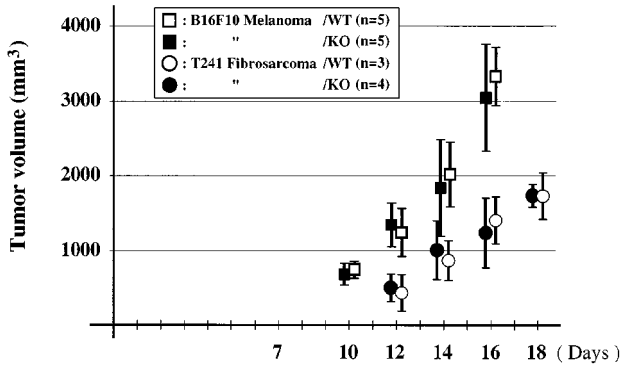

Fig. 11. Growth of B16F10 melanoma and T241 fibrosarcoma tumors in wild-type (open symbols) and collagen XVIII null (filled symbols) mice. Vertical bars represent standard deviations in tumor volume.

In Bruch's membrane, the clustering of gold particles was particularly evident in tangential sections, where the clusters of gold particles were distributed on an almost uniform lattice (Figure 9B) and appeared to be co-localized with collagen fibrils in the tissue separating pigment epithelial and endothelial basement membranes. Along the pigment epithelial cells, robust labeling was seen on both sides of the lamina densa (Figure 9B). In this respect, this basement membrane differs from all other basement membranes we have examined. In the pigment epithelial basement membrane, collagen XVIII molecules must be symmetrically organized along the lamina densa, with the N-terminal regions exposed on both the epithelial (retinal) side and the choriocapillary side. This suggests that collagen XVIII may be of particular significance for the structure, function or turnover of the pigment epithelial basement membrane.

Ultrastructural abnormalities along the inner limiting membrane of collagen XVIII null mice

Comparison of the ultrastructure of ocular tissues in wild-type and *Col18a1*$^{-/-}$ mice showed no detectable differences in regions that contain collagen XVIII, with the exception of the inner limiting membrane. Along the inner limiting membrane of wild-type eyes, collagenous fibrils, surrounded by non-fibrillar material, were present at the periphery of the vitreous and in close proximity to the membrane (Figure 10). In areas where the fibrils appeared to 'insert' into the membrane, heavy labeling was seen with gold-labeled antibodies against NC11(XVIII) (Figure 8C). In the majority of sections of *Col18a1*$^{-/-}$ eyes, no fibrils were seen in the peripheral regions of the vitreous, and areas of fibril 'insertions' into the inner limiting membrane were difficult to find (Figure 10B). The limiting membrane was otherwise identical in wild-type and *Col18a1*$^{-/-}$ eyes.

No difference in tumor growth in wild-type and collagen XVIII null mice

Since endostatin has been shown to have antiangiogenic and antitumor effects in mice when administered as a recombinant protein (O'Reilly *et al*., 1997), we inoculated wild-type and collagen XVIII null mice with B16F10 melanoma and T241 fibrosarcoma tumor cells and followed the growth of tumors over a period of 18 days. No difference in growth rate was observed for either tumor type (Figure 11). Thus, the physiological levels of endostatin in wild-type mice are insufficient to exert a negative effect on the growth of melanomas and fibrosarcomas.

Discussion

Role of collagen XVIII/endostatin in ocular angiogenesis

The hyaloid vessels of the eye normally regress according to a developmental program (Ito and Yoshioka, 1999). The exact mechanisms for the regression are not known, but apoptosis and tissue macrophages are likely to be involved (Lang and Bishop, 1993; Lang *et al*., 1994; Diez-Roux and Lang, 1997; Mitchell *et al*., 1998; Zhu *et al*., 2000). In collagen XVIII null mice, VHP persist far beyond the time when they have completely disappeared in wild-type mice. This suggests that collagen XVIII/endostatin plays a role in the normal regression of the VHP. A similar persistence of the hyaloid vasculature has been observed in mice carrying a transgene that allows elimination of macrophages in the eye (Lang and Bishop, 1993). This suggests that macrophages and collagen XVIII/endostatin may co-operate in the normal regression of VHP. Future studies are needed to examine the nature of this potential co-operation.

The delayed regression of the VHP in collagen XVIII null mice is probably the cause of abnormal vascularization of the retina. As mentioned above, postnatal retinal vascularization in rodents is driven by hypoxia-induced VEGF expression in neuroglial cells (Alon *et al*., 1995; Stone *et al*., 1995; Benjamin *et al*., 1998; Yancopoulos *et al*., 2000). Exposure to hyperoxia has been shown to repress VEGF expression (Alon *et al*., 1995; Pierce *et al*., 1996; Stone *et al*., 1996); thus, the persistence of large hyaloid vessels on the anterior retinal surface in the collagen XVIII null mice would lead to higher local oxygen levels than in wild-type eyes, and may explain the lower levels of VEGF (Figure 5). The variability in retinal vascular patterns between different individual mutant mice (see Figure 4) could be a consequence of variability in the number and precise location of VHP (see Figure 2). Even in mutant mice where the hyaloid vessels do eventually disappear, the retinal vessels may be abnormal, since it has

been demonstrated that a return to normoxia, following a brief period of hyperoxia, leads to an abnormal burst of VEGF production and outgrowth of vessels in an abnormal pattern (Yancopoulos *et al*., 2000).

The delayed regression of hyaloid vessels on the surface of the retina in collagen XVIII-deficient mice is in striking contrast to the normal disappearance of the vessels on the posterior surface of the lens. This suggests that mechanisms controlling regression of vessels within the TVL and VHP are different. It has been suggested that apoptosis of endothelial cells within the TVL is triggered by a rapid thickening of the posterior lens capsule that separates the endothelial cells from VEGF-producing cells within the lens (Mitchell *et al*., 1998). This attenuation of the VEGF survival signal may be further accentuated by binding of VEGF to heparan sulfate proteoglycans within the lens capsule.

Abnormalities along the inner limiting membrane in collagen XVIII null mice

Co-localization of gold-labeled NC11(XVIII) antibodies with regions where collagen fibrils are 'inserted' into the inner limiting membrane, combined with reduced numbers of vitreous fibrils along the inner limiting membrane in many sections of *Col18a1*$^{-/-}$ eyes, suggests that collagen XVIII/endostatin is important for the connection between the collagenous matrix of the vitreous and the inner limiting membrane of the retina. In this location in the eye, collagen XVIII/endostatin may function primarily as a component of an anchoring complex between collagen fibrils and the basement membrane. In contrast, the absence of collagen XVIII/endostatin in skin and cornea does not result in separation of the lamina densa from the underlying matrix, and other components must play a compensatory role. Why the inner limiting membrane region should be different in this respect may be related to the unique composition of the matrix that underlies the inner limiting membrane. In skin, cornea and around blood vessels in all other locations, the matrix contains fibrils of collagens I, III and V, and other components associated with such fibrils. In the vitreous, the fibrillar structure is almost identical to that of cartilage, with collagens II, IX and XI. The inner limiting membrane is therefore unique among basement membranes in that it is connected to a cartilage-like matrix, and it may not contain the components that can compensate for the loss of collagen XVIII/endostatin in other basement membranes. This unique connection of the inner limiting membrane to a cartilage-like matrix may also explain why the localization of gold particles associated with anti-NC11(XVIII) antibodies is different for this basement membrane compared with epidermal and corneal basement membranes (Figure 8). The posterior lens capsule is also connected to this cartilage-like matrix, but is thicker and in many respects not comparable to other basement membranes; thus, it is not surprising that we found no abnormalities along this membrane in *Col18a1*$^{-/-}$ eyes.

Phenotypic consequences of lack of collagen XVIII/endostatin in humans

In DNA from patients with recessively inherited Knobloch syndrome, Sertié *et al*. (2000) found a splice site mutation that causes premature termination of the short form of collagen XVIII. While affected individuals are still able to synthesize the long variants, they are likely to be functionally null for the short form of collagen XVIII. Mutations that cause premature termination of all variants have been identified in additional Knobloch patients, and these patients appear to have the same phenotype as patients with the splice site mutation (M.R.Passos-Bueno, personal communication). This suggests that the phenotype of Knobloch patients—high myopia, vitreoretinal degeneration with retinal detachment, macular abnormalities and occipital encephalocele—is due to loss of collagen XVIII function.

It is conceivable that the Knobloch phenotype may be a consequence of blood vessel-associated abnormalities that somehow affect the expression and/or assembly of collagens II and XI, the major components of vitreous fibrils. In patients with Stickler-like syndromes, mutations in *COL2A1* or *COL11A1* cause ocular abnormalities that are similar to those seen in Knobloch syndrome (Mundlos and Olsen, 1997; Annunen *et al*., 1999). An alternative possibility is that structural changes at the vitreous-inner limiting membrane interface cause the high myopia, vitreoretinal degeneration and retinal detachment of Knobloch syndrome. In support of this alternative, which we favor, is the loss of connectivity between the vitreal fibrils and the inner limiting membrane in most sections of *Col18a1*$^{-/-}$ eyes, reflecting a collapse of the vitreous. During the first postnatal days, the secondary vitreous forms in the space between the inner limiting membrane and the VHP. Consequently, this changes the VHP position and compresses it centrally around the hyaloid artery, and apparently pushes the VHP towards the lens (Bischoff *et al*., 1983; Ito and Yoshioka, 1999). During dissection of postnatal eyes in preparation for whole-mount staining of retinal vessels, it was noted that hyaloid vessels appeared more tightly adhered to the retina in *Col18a1*$^{-/-}$ eyes than in wild-type eyes, and hyaloid vessel profiles could be seen in close association with the retinal surface in sections of *Col18a1*$^{-/-}$ eyes (see Figure 2). Thus, we believe that absence of collagen XVIII causes structural changes in the inner limiting membrane or the basement membrane of the VHP, resulting in abnormal adhesion of these vessels to the retina. In combination with a collapse of the vitreous and its retraction from the retina, this could lead to retinal detachment.

The macular degeneration associated with Knobloch syndrome is likely the result of abnormalities in the retinal vasculature or age-related changes in the pigment epithelial layer as a consequence of alterations in Bruch's membrane. The encephalocele may be a human-specific consequence of collagen XVIII mutations, since we have not been able to detect any abnormalities in the posterior part of the brain or skull in the knockouts. X-ray imaging of wild-type and mutant animals (not shown) did not reveal any abnormalities in the thickness of the skull in homozygous knockouts, nor could we detect any changes in pial basement membranes stained with anti-collagen IV antibodies (not shown).

Antitumor effects of endostatin

The lack of any difference in the rate of growth of B16F10 melanoma and T241 fibrosarcomas in wild-type mutant mice suggests that physiological levels of endostatin are

insufficient to exert detectable antitumor effects in mice. This is not particularly surprising, since most studies where such effects have been reported have involved much higher concentrations of recombinant endostatin (O'Reilly *et al*., 1997). In studies that used particularly small amounts of endostatin it is also likely that the concentrations exceeded the physiological levels because of local delivery (Yamaguchi *et al*., 1999; Joki *et al*., 2001; Read *et al*., 2001).

Materials and methods

Gene targeting and generation of mutant mice

A mouse genomic library (Stratagene, La Jolla, CA) was screened with the α1(XVIII) collagen cDNA clone mc3a (Oh *et al*., 1994). A genomic clone, P4-1, was characterized and shown to contain 22 exons corresponding to exons 17–38 of the *Col18a1* gene. A 12 kb *Not*I–*Kpn*I fragment of P4-1 was used to make a replacement vector. A *neo*^{R} cassette (containing the PGK promoter, the neomycin resistance gene and a polyadenylation signal) was ligated into a *Sal*I site within exon 30 that encodes part of the COL5 domain (Figure 1A and B). J1 embryonice stem (ES) cells were transfected with the replacement vector by electroporation and selected in G418-containing medium as described previously (Li *et al*., 1992). The genotype of G418-resistant clones was analyzed by Southern blotting. A correctly targeted clone was injected into C57BL/6J blastocysts to generate chimeric mice (Li *et al*., 1992). Chimeric mice were bred either to 129 Sv/J or C57BL/6J mice to generate 129 Sv inbred or F_1 hybrid heterozygous knockout mice, respectively. The F_1 heterozygous mice were backcrossed to C57BL/6J mice for 15 generations to generate the C57BL/6J inbred knockout lines.

Genotyping, Southern blot analysis, PCR and northern blot analysis

Genomic DNAs, obtained from mouse tails by proteinase K digestion (Laird *et al*., 1991), were digested with *Eco*RI, electrophoresed, and blotted to positively charged nylon membranes (Hybond N$^+$; Amersham Pharmacia Biotech, Piscataway, NJ). Hybridization was carried out with a *Kpn*I–*Eco*RI probe, chosen from a gene region outside the construct (Figure 1B). The wild-type *Col18a1* allele gave a 19 kb band. Since an *Eco*RI site is located within the *neo*^{R} cassette, mutated alleles containing the *neo*^{R} cassette as a result of homologous recombination gave a 6 kb band.

Sense (SW) and antisense (RW) primers, flanking the *Sal*I site used to insert the *neo*^{R} cassette, and a sense primer within the *neo*^{R} cassette (SN) were used for detection of both alleles by PCR (Figure 1B and C). The sequence of SW was 5′-TAGAGCTGAATAACACCTG-3′, RW was 5′-CCTCATGCTGAACCCAAGG-3′ and SN was 5′-CAGCGC-ATCGCCTTCTAT-3′. After 3 min of denaturation at 95°C, the amplification conditions were as follows: 30 s denaturing at 94°C, 45 s annealing at 56°C and 1 min extension at 72°C for 33 cycles, followed by 10 min of final extension at 72°C. The PCR products were analyzed by electrophoresis through 0.8% agarose. PCR with the SW/RW primer combination gave a 1.0 kb product with the wild-type allele, and the combination of SN/RW primers with the mutated allele gave a 0.65 kb product.

Total RNAs were prepared from whole embryos or tissues of adult mice as described previously (Chirgwin *et al*., 1979). Electrophoresis through a 1.0% agarose gel in the presence of formamide/formaldehyde was followed by transfer to positively charged nylon membranes (Hybond N$^+$). ^{32}P-labeled probes were from the 3′ untranslated and endostatin region of *Col18a1* mRNA and from the 5′ region, covering exons 4–7.

Assay of endostatin in plasma

For measurements of plasma concentrations of endostatin and endostatin-like fragments, blood was collected by heart puncture from 3- to 4-month-old wild-type, heterozygous and homozygous knockout mice. Concentrations of endostatin-containing collagen XVIII fragments were determined using a competitive enzyme-linked immunoassay method (Accucyte; CytImmune Sciences, Inc., College Park, MD), in which complexes of serum endostatin, biotinylated mouse endostatin and rabbit anti-mouse endostatin antibodies are captured on plates pre-coated with goat anti-rabbit antibodies. The sensitivity of the assay is ~2 ng/ml and the assay is linear to 500 ng/ml.

Whole-mount preparations and staining of developing blood vessels in retina

On postnatal day 4, mice were killed and eye globes were placed in PFA fixative [4% paraformaldehyde in phosphate-buffered saline (PBS) pH 7.2]. The globes were incised through the cornea with a razor blade, the lens and the hyaloid vasculature were removed, the membranes were enucleated around the retinal cup under a dissection microscope, and the retinas were fixed in the PFA fixative for 1 h at room temperature. After a 1 h incubation in –20°C methanol, the retinas were treated for 2 h in a blocking buffer [50% fetal calf serum (FCS) and 1% Triton X-100 in PBS] at room temperature and subsequently incubated with primary antibodies (rabbit anti-mouse type IV collagen polyclonal antibody; Chemicon International Inc., Temecula, CA; 1:200 in 10% FCS, PBS) overnight at 4°C. The retinas were washed four times for 5 min with PBS, incubated for 3–4 h with secondary antibodies (CY3-conjugated polyclonal swine anti-rabbit; Amersham Pharmacia Biotech; 1:300 in 10% FCS, PBS), washed four times for 5 min with PBS, mounted with Immu-mount (Shandon, Pittsburgh, PA), and examined in an epifluorescence microscope (Leitz Aristoplan; Leitz, Wetzlar, Germany).

Histological examination of eye vasculature and immunohistochemistry

For histological examination of eye vasculature, mice were killed on postnatal days 0.5, 4, 8, 16 and 24. After fixation in phosphate-buffered formalin (10%, pH 7.0) overnight at room temperature and embedding in paraffin, eyes were sectioned from the surface of horizontally oriented globes under the plane of the optic nerve head.

HE-stained sections were observed under a light microscope and the number of hyaloid capillaries in primary vitreous (VHP) and vessels around the developing lens (TVL) were counted at postnatal days 0.5, 4, 8, 16 and 24. Rudiments of regressing vessels were not counted. The number of vessels were determined from at least eight horizontal planes of each eye. Quantitative evaluation of the vessel profiles was performed on horizontally oriented sections. The statistical difference between means was analyzed using the Mann–Whitney *U*-test.

For immunohistochemical detection of collagen XVIII and collagen IV in basement membranes of wild-type and mutant mice, sections of PFA-fixed (4% PFA in phosphate buffer pH 7.4) and paraffin-embedded tissues were stained with polyclonal anti-collagen antibodies following treatment with proteinase XXIV (Sigma) and blocking with 5 or 10% goat serum in PBS. For collagen XVIII, affinity-purified, polyclonal rabbit antibodies against a 298 amino acid residue recombinant fragment (common to all forms of collagen XVIII) from the N-terminal NC11 domain of the protein were prepared. Collagen IV antibodies were from Chemicon International, Inc., and used at 1:800 dilution. Secondary antibodies were biotinylated goat anti-rabbit IgG (Sigma, St Louis, MO); detection was with peroxidase-labeled streptavidin and DAB reagent (BioGenex, San Ramon, CA). Counterstaining was with methylgreen. For immunofluorescence with collagen XVIII antibodies, an FITC-labeled secondary anti-rabbit antibody (Sigma) was used.

For detection of macrophages within the vitreous, sections of PFA-fixed and paraffin-embedded tissues were stained with anti-mouse Mac-3 monoclonal antibody (BD PharMingen, San Diego, CA).

In situ hybridization and quantitative PCR

For determination of VEGF expression by *in situ* hybridization, eyes from 1-day-old wild-type and *Col18a1*$^{-/-}$ mice were fixed, embedded in OCT compound, and sectioned as described previously (Gong *et al*., 2001). Murine VEGF antisense probes were synthesized to cover 450 bp of cDNA (a gift from B.Cohen, Weizmann Institute, Israel). Digoxigenin-11-UTP-labeled single-strand ribo-probes were prepared as described previously (Gong *et al*., 2001), and hybridization was carried out overnight in 50% formamide at 52°C. Washing, detection, staining and mounting of slides were carried out as described previously (Böhme *et al*., 1995).

For quantitative PCR, retinas were dissected from wild-type and mutant eyes at postnatal day 4 and placed in RNA later solution (Qiagen Inc., Valencia, CA). Total RNA was isolated, using the Qiagen RNeasy kit, according to the manufacturer's protocol, except that homogenization included vortexing, followed by aspiration through a 20-gauge needle. cDNA was made with Qiagen Sensicript RT kit. VEGF mRNA levels were measured with the ABI 7700 Sequence Detection System using TaqMan chemistry and forward and reverse primers 5′-GATCCG-CAGACGTGTAAATGTTC-3′ and 5′-TTAACTCAAGCTGCCTC-GCC-3′, respectively. The VEGF amplicon was detected using the bifunctional fluorogenic probe 5′-Fam-TGCAAAAACACAGACTCG-CGTTGCA-Tamra-3′. VEGF mRNA levels were normalized to levels of

18S mRNA quantified in the same samples using the forward and reverse primers 5′-TGGTTGCAAAGCTGAAACTTAAAG-3′ and 5′-AGTCAA-ATTAAGCCGCAGGC-3′, respectively. The probe for the 18S amplicon was 5′-Vic-CCTGGTGGTGCCCTTCCGTCA-Tamra-3′.

Electron microscopy

Three wild-type and three *Col18a1*$^{-/-}$ littermates were killed on postnatal day 10; seven wild-type and five *Col18a1*$^{-/-}$ mice were 4 months or older. For electron microscopy without immunolabeling, whole eyes were fixed at room temperature for 1–2 h in 1.25% paraformaldehyde and 0.03% picric acid in 0.1 M cacodylate buffer pH 7.4. After further dissection, specimens were postfixed in 1% osmium tetroxide and 1.5% potassium ferrocyanide at room temperature for 1 h, stained *en bloc* in 1% uranyl acetate for 30 min, and embedded in Epon (EMbed 812; Electron Microscopy Sciences, Fort Washington, PA). Ultrathin sections were contrasted with uranyl acetate and lead citrate and examined in a 1200EX JEOL electron microscope.

For immunolabeling, *en bloc* labeling was used as described previously (Sakai and Keene, 1994). Eyes were lightly prefixed in 0.1% glutaraldehyde, 4% paraformaldehyde in 0.1 M cacodylate buffer pH 7.4, immunolabeled *en bloc* by immersing in primary antibody, rinsed extensively in PBS, immersed in goat anti-rabbit 1 nm gold conjugate (Amersham Pharmacia Biotech) diluted 1:3, and rinsed extensively in PBS. The 1 nm gold particles in some instances were enhanced using the Nanoprobe GEEM gold enhance kit (Nanoprobes, Inc., Yaphank, NY). This was followed by fixation in 1.5% glutaraldehyde, 1.5% paraformaldehyde containing 0.05% tannic acid in 0.1 M cacodylate buffer and fixation in 1% osmium tetroxide before embedding in Spurrs epoxy (Ladd Research, Williston, VT). Ultrathin sections were contrasted with uranyl acetate and lead citrate prior to evaluation in a Phillips 410LS electron microscope.

Tumor growth assay

To ensure uniformity of genetic backgrounds of wild-type and mutant littermates, *Col18a1*$^{-/-}$ mice were backcrossed with C57BL/6 mice for 15 generations. Cells from B16F10 melanoma (provided by M.O'Reilly) and T241 fibrosarcoma (provided by T.Tanaka) were cultured in high glucose DMED medium (Irvine Scientific, Santa Ana, CA) containing 5% fetal bovine serum (FBS) (Cascade Biologics, Portland, OR), 100 U/ml penicillin and 100 µg/ml streptomycin. Following trypsinization, 5×10^6 B16F10 melanoma cells and 1×10^6 T241 fibrosarcoma cells in 0.1 ml PBS were injected into a subcutaneous dorsal site of wild-type and collagen XVIII null littermates of both sexes.

The tumors became visible ~7 days after inoculation, and their sizes were measured with a caliper on days 10, 12, 14, 16 and 18. The shortest (d_1) and longest (d_2) diameters were measured (in mm) along two perpendicular axes, and the volume was calculated using the formula $V = 0.52 \times d_1 \times d_1 \times d_2$.

Acknowledgements

We thank Yulia Pittel, Sofiya Plotkina, Byron Simpson, Päivi Tuomaala, Sara F.Tufa and Maria Erickson for excellent secretarial and technical assistance. Drs E.Boye, M.R.dos Santos e Passos-Bueno, M.Vikkula, and U.Zätterström are thanked for helpful comments. This work was supported by NIH grants AR38819 and AR36820, grants from the Finnish Centre of Excellence Programme (2000–2005) of the Academy of Finland (44843), the Sigrid Juselius Foundation, Boehringer Ingelheim Fonds, Shriners Hospital for Children, EntreMed, Inc. (Rockville, MD), and FibroGen Inc. (South San Francisco, CA).

References

Alon,T., Hemo,I., Itin,A., Pe'er,J., Stone,J. and Keshet,E. (1995) Vascular endothelial growth factor acts as a survival factor for newly formed retinal vessels and has implications for retinopathy of prematurity. *Nature Med.*, **1**, 1024–1028.

Annunen,S. *et al*. (1999) Splicing mutations of 54-bp exons in the COL11A1 gene cause Marshall syndrome, but other mutations cause overlapping Marshall/Stickler phenotypes. *Am. J. Hum. Genet.*, **65**, 974–983.

Benjamin,L.E., Hemo,I. and Keshet,E. (1998) A plasticity window for blood vessel remodelling is defined by pericyte coverage of the preformed endothelial network and is regulated by PDGF-B and VEGF. *Development*, **125**, 1591–1598.

Bischoff,P.M., Wajer,S.D. and Flower,R.W. (1983) Scanning electron microscopic studies of the hyaloid vascular system in newborn mice exposed to O_2 and CO_2. *Graefes Arch. Clin. Exp. Ophthalmol.*, **220**, 257–263.

Böhme,K., Li,Y., Oh,S.P. and Olsen,B.R. (1995) Primary structure of the long and short splice variants of mouse collagen XII and their tissue-specific expression during embryonic development. *Dev. Dyn.*, **204**, 432–445.

Chirgwin,J.M., Przybyla,A.E., MacDonald,R.J. and Rutter,W.J. (1979) Isolation of biologically active ribonucleic acid from sources enriched in ribonuclease. *Biochemistry*, **18**, 5294–5299.

Diez-Roux,G. and Lang,R.A. (1997) Macrophages induce apoptosis in normal cells *in vivo*. *Development*, **124**, 3633–3638.

Felbor,U., Dreier,L., Bryant,R., Ploegh,H.L., Olsen,B.R. and Mothes,W. (2000) Secreted cathepsin L generates endostatin from collagen XVIII. *EMBO J.*, **19**, 1187–1194.

Ferreras,M., Felbor,U., Lenhard,T., Olsen,B.R. and Delaisse,J. (2000) Generation and degradation of human endostatin proteins by various proteinases. *FEBS Lett.*, **486**, 247–251.

Gong,Y. *et al*. (2001) LDL receptor-related protein 5 (LRP5) affects bone accrual and eye development. *Cell*, **107**, 513–523.

Halfter,W., Dong,S., Schurer,B. and Cole,G.J. (1998) Collagen XVIII is a basement membrane heparan sulfate proteoglycan. *J. Biol. Chem.*, **273**, 25404–25412.

Halfter,W., Dong,S., Schurer,B., Osanger,A., Schneider,W., Ruegg,M. and Cole,G.J. (2000) Composition, synthesis and assembly of the embryonic chick retinal basal lamina. *Dev. Biol.*, **220**, 111–128.

Ito,M. and Yoshioka,M. (1999) Regression of the hyaloid vessels and pupillary membrane of the mouse. *Anat. Embryol.*, **200**, 403–411.

Joki,T., Machluf,M., Atala,A., Zhu,J., Seyfried,N.T., Dunn,I.F., Abe,T., Carroll,R.S. and Black,P.M. (2001) Continuous release of endostatin from microencapsulated engineered cells for tumor therapy. *Nature Biotechnol.*, **19**, 35–39.

Laird,P.W., Zijderveld,A., Linders,K., Rudnicki,M.A., Jaenisch,R. and Berns,A. (1991) Simplified mammalian DNA isolation procedure. *Nucleic Acids Res.*, **19**, 4293.

Lang,R.A. and Bishop,J.M. (1993) Macrophages are required for cell death and tissue remodeling in the developing mouse eye. *Cell*, **74**, 453–462.

Lang,R., Lustig,M., Francois,F., Sellinger,M. and Plesken,H. (1994) Apoptosis during macrophage-dependent ocular tissue remodelling. *Development*, **120**, 3395–3403.

Li,E., Bestor,T.H. and Jaenisch,R. (1992) Targeted mutation of the DNA methyltransferase gene results in embryonic lethality. *Cell*, **69**, 915–926.

Mitchell,C.A., Risau,W. and Drexler,H.C. (1998) Regression of vessels in the tunica vasculosa lentis is initiated by coordinated endothelial apoptosis: a role for vascular endothelial growth factor as a survival factor for endothelium. *Dev. Dyn.*, **213**, 322–333.

Mundlos,S. and Olsen,B.R. (1997) Heritable diseases of the skeleton. Part II: Molecular insights into skeletal development-matrix components and their homeostasis. *FASEB J.*, **11**, 227–233.

Muragaki,Y., Timmons,S., Griffith,C.M., Oh,S.P., Fadel,B., Quertermous,T. and Olsen,B.R. (1995) Mouse *Col18a1* is expressed in a tissue-specific manner as three alternative variants and is localized in basement membrane zones. *Proc. Natl Acad. Sci. USA*, **92**, 8763–8767.

Oh,S.P., Kamagata,Y., Muragaki,Y., Timmons,S., Ooshima,A. and Olsen,B.R. (1994) Isolation and sequencing of cDNAs for proteins with multiple domains of Gly-X-Y repeats identify a novel family of collagenous proteins. *Proc. Natl Acad. Sci. USA*, **91**, 4229–4233.

O'Reilly,M.S. *et al*. (1997) Endostatin: an endogenous inhibitor of angiogenesis and tumor growth. *Cell*, **88**, 277–285.

Pierce,E.A., Foley,E.D. and Smith,L.E. (1996) Regulation of vascular endothelial growth factor by oxygen in a model of retinopathy of prematurity [published erratum appears in *Arch. Ophthalmol.* (1997) **115**, 427]. *Arch. Ophthalmol.*, **114**, 1219–1228.

Read,T.A., Sorensen,D.R., Mahesparan,R., Enger,P.O., Timpl,R., Olsen,B.R., Hjelstuen,M.H., Haraldseth,O. and Bjerkvig,R. (2001) Local endostatin treatment of gliomas administered by micro-encapsulated producer cells. *Nature Biotechnol.*, **19**, 29–34.

Rehn,M. and Pihlajaniemi,T. (1994) α1(XVIII), a collagen chain with frequent interruptions in the collagenous sequence, a distinct tissue distribution and homology with type XV collagen. *Proc. Natl Acad. Sci. USA*, **91**, 4234–4238.

Saarela,J., Rehn,M., Oikarinen,A., Autio-Harmainen,H. and Pihlajaniemi,T. (1998) The short and long forms of type XVIII

collagen show clear tissue specificities in their expression and location in basement membrane zones in humans. *Am. J. Pathol.*, **153**, 611–626.

Sakai,L.Y. and Keene,D.R. (1994) Fibrillin: monomers and microfibrils. *Methods Enzymol.*, **245**, 29–52.

Sasaki,T., Fukai,N., Mann,K., Gohring,W., Olsen,B.R. and Timpl,R. (1998) Structure, function and tissue forms of the C-terminal globular domain of collagen XVIII containing the angiogenesis inhibitor endostatin. *EMBO J.*, **17**, 4249–4256.

Sertié,A.L., Sossi,V., Camargo,A.A., Zatz,M., Brahe,C. and Passos-Bueno,M.R. (2000) Collagen XVIII, containing an endogenous inhibitor of angiogenesis and tumor growth, plays a critical role in the maintenance of retinal structure and in neural tube closure. *Hum. Mol. Genet.*, **9**, 2051–2058.

Stone,J., Itin,A., Alon,T., Pe'er,J., Gnessin,H., Chan-Ling,T. and Keshet,E. (1995) Development of retinal vasculature is mediated by hypoxia-induced vascular endothelial growth factor (VEGF) expression by neuroglia. *J. Neurosci.*, **15**, 4738–4747.

Stone,J., Chan-Ling,T., Pe'er,J., Itin,A., Gnessin,H. and Keshet,E. (1996) Roles of vascular endothelial growth factor and astrocyte degeneration in the genesis of retinopathy of prematurity. *Invest. Ophthalmol. Vis. Sci.*, **37**, 290–299.

Wen,W., Moses,M.A., Wiederschain,D., Arbiser,J.L. and Folkman,J. (1999) The generation of endostatin is mediated by elastase. *Cancer Res.*, **59**, 6052–6056.

Yamaguchi,N. *et al*. (1999) Endostatin inhibits VEGF-induced endothelial cell migration and tumor growth independently of zinc binding. *EMBO J.*, **18**, 4414–4423.

Yancopoulos,G.D., Davis,S., Gale,N.W., Rudge,J.S., Wiegand,S.J. and Holash,J. (2000) Vascular-specific growth factors and blood vessel formation. *Nature*, **407**, 242–248.

Zhu,M., Madigan,M.C., van Driel,D., Maslim,J., Billson,F.A., Provis, J.M. and Penfold,P.L. (2000) The human hyaloid system: cell death and vascular regression. *Exp. Eye Res.*, **70**, 767–776.

Received October 31, 2001; revised January 31, 2002; accepted February 5, 2002